Acta Ciencia Indica, Vol. XL C, No. 1, 31 (2014)

JUDD-OFELT ANALYSIS OF DYSPROSIUM IN SOL GEL SILICA

JEENA THOMAS, AJITH VERGHESE GEORGE

Department of Chemistry, Mar Ivanios College, Thiruvananthapuram (Kerala), India

AND

VINOY THOMAS

Department of Physics, Christian College, Chengannur – 689 122, Kerala (India)

RECEIVED : 7 January, 2014

Preparation and Judd-Ofelt (JO) analysis of Dysprosium doped sol gel silica glass is reported. The calculated values of the JO parameters are utilized to evaluate , various radiative parameters such as electric dipole line strengths (S_{ed}), radiative transition probabilities (A_{RAD}), radiative lifetimes (τ_{RAD}), fluorescence branching ratios (β_R) and the integrated absorption cross sections (σ_a) for stimulated emission from various excited states of the rare earth ion. The analysis reveals the potential of ${}^4F_{9/2} \rightarrow {}^6H_{13/2}$ and ${}^4F_{9/2} \rightarrow {}^6H_{15/2}$ transitions of Dy^{3+} ion for optical applications.

KEYWORDS: so-gel materials, Judd-Ofelt theory, optical materials.

INTRODUCTION

Silica glasses containing rare earth ions as luminescent centers are of great deal of interest for their unique optical properties [Maria *et al* (2009), You *et al* (2014)]. Rare earth ions have number of efficient and narrow emission lines in the visible and NIR wavelength region whose position is insensitive to their matrices due to the shielding effect of 5*s* and 5p electrons. Most often, research efforts have concentrated on fluoride, tellurite and chalcogenide glass systems because of their lower phonon energies compared to oxide glasses. On the contrary, oxide glasses are more suitable for practical applications due to their high chemical durabilities and thermal stabilities. In oxide glasses, silicate glasses are one of the most popular glass hosts for making optical fiber lasers and amplifiers. The potential advantage of the sol-gel method for preparing optical materials includes obtaining new chemical compositions, better purity and more convenient processing conditions [Coasta *et al* 1996, Jeena *et al* 2013, Paulose *et al* 2002, Thomas *et al* 1992, Vinoy *et al* 2005]. Recent studies of rare earth ions in different environments indicate that Dy^{3+} doped systems are known as a two primary color (yellow/blue) luminescent materials [Joanna 2010]. In comparison with other rare earth ions, number studies on Dy^{3+} ions in sol-gel glasses is limited. In this context, optical analysis of Dy^{3+} ions doped sol gel glass deserves special attention and importance.

EXPERIMENTAL

Silica sols containing 2 equivalent mol% Dy_2O_3 were prepared from tetraethylorthosilicate (TEOS) (Flukapurum grade), $Dy(NO_3)_3.6H_2O$ (Merck), doubly distilled deionised water and high purity HNO_3 and NH_4OH. The desired amount of $Dy(NO_3)_3.6H_2O$ dissolved in deionised water in the presence of HNO_3 was poured in TEOS under stirring at room temperature. The TEOS/H_2O/HNO_3 molar ratio was 1:14:0.01. The pH of the sols was adjusted to a value of 3 by adding NH_4OH. The sols were cast in petridishes. The gels were aged for one week at room temperature. Transparent crack free dried monolithic gels were obtained after drying for 14 days in air oven at 60° ± 2°C. The gels were heated at different temperatures ranging from 200-900°C in a programmable furnace with the rate of 3°C per hour. Transparent crack free and bubble free gels (diameter 30-35 mm, thickness 2-2.5 mm) were reproducibly obtained. The following equations give the simplified mechanisms leading to the gelation of the precursor solution

$$\equiv Si\text{-}OC_2H_5 + H_2O \rightarrow \equiv Si\text{–}OH + C_2H_5OH \qquad \ldots (1)$$

$$\equiv Si\text{–}OH + HO\text{-}Si \rightarrow \equiv Si\text{–}O\text{-}Si\equiv + H_2O \qquad \ldots (2)$$

$$\equiv Si\text{–}OH + H_5C_2O\text{-}Si\equiv \rightarrow \equiv Si\text{–}O\text{-}Si\equiv + C_2H_5OH \qquad \ldots (3)$$

Mechanism (1) represents hydrolysis reaction and mechanisms (2) and (3) represent condensation reactions. Simultaneously a cluster-cluster aggregation process takes place as the sol converts to gel. The rare earth nitrates become increasingly entangled and ultimately trapped within the growing clusters, which make the dopant ions disperse in the derived gel at a molecular level. Optical spectra of the gels and heat treated samples were recorded with UV-VIS (Schimadzu 5401) spectrophotometer.

RESULTS AND DISCUSSION

Figure.1 shows the typical absorption spectra of 2mol% Dy_2O_3 doped silica gel fired at 900°C. Figure 2 shows the energy level diagram of Dy^{3+} in silica matrix. All the spectra of rare earth ions arise from the intra-configuration transitions within the 4f shell [Thomas et al 2005]. The electronic transitions of the trivalent lanthanides can be electric dipole, magnetic dipole or electric quadrupole in nature [Jayasankar *et al* 1997]. Neglecting higher multipole mechanisms such as electric quadrupole transitions, oscillator strength (f) can be regarded as a sum of the electric dipole (f_{ed}) and magnetic dipole (f_{md}) contributions, *i.e.*,

$$F = f_{ed} + f_{md} \qquad \ldots (1)$$

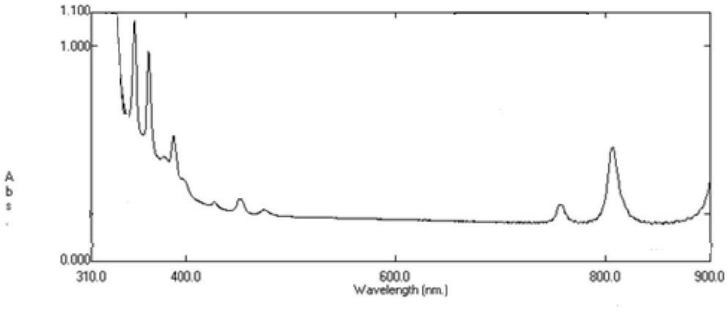

Fig. 1. Optical absorption spectra of Dy^{3+} in silica matrix

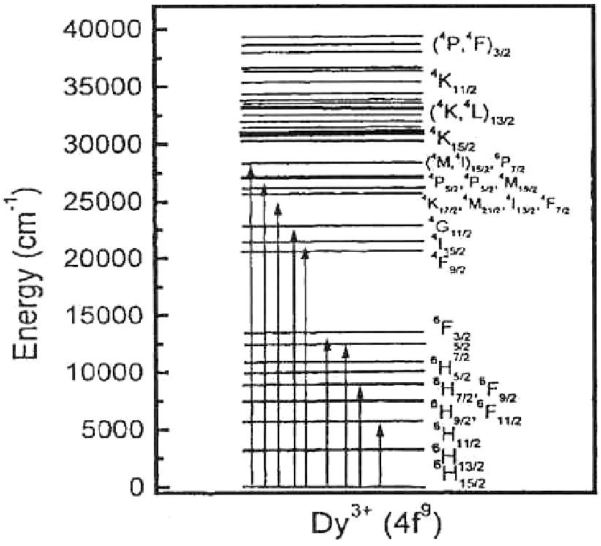

Figure 2. Energy level diagram of Dy^{3+} ions [31]

It is well known that for rare earth ions, the intermanifold line strength of magnetic dipole (md) transitions is much less than the line strength of electric dipole (ed) transitions $(S_{JJ'}^{md} << S_{JJ'}^{ed})$. The experimentally measured oscillator strengths of various absorption transitions of Dy^{3+} ion in the present glassy systems are found to be in good agreement with that of other oxide systems (Table 1). Oscillator strength (*f*) can be expressed in terms of the molar extinction coefficient (ε), and the energy of the transition in wave number (ν) by the relation [Gijo *et al* 2006].

$$f_{\exp} = 4.32 \times 10^{-9} \int \varepsilon(\nu)\, d\nu \qquad \ldots (2)$$

Table 1. Oscillator strengths (10^{-6}) and electric dipole line strengths (10^{-20}) of all the observed transitions of Dy^{3+} in silica matrix.

Transitions from $^6H_{15/2}$	**Pure SiO_2**	
	$f_{mes}(10^{-6})$	**S_{ed} (10^{-22}) cm^2**
$^6P_{7/2}$	2.94	1.31
$^6P_{5/2}$	2.31	1.06
$^4F_{7/2}$	0.984	0.484
$^4I_{15/2}$	0.622	0.355
$^6F_{5/2}$	1.13	1.08
$^6F_{7/2}$	6.27	6.41

The absorption properties of rare earth ions are best distinguished in the context of Judd-Ofelt (JO) theory [Judd BR 1962, Ofelt GS 1962]. According to JO theory $4f \rightarrow 4f$ transitions of a rare earth ion can be described as a simple linear combination of the so-called JO parameters Ω_λ ($\lambda = 2, 4, 6$). The coefficients of each linear combination of Ω_λ are independent of the host and are determined by the fundamental nature of the 4*f* wave functions and the particular transitions at hand.

According to J-O theory

$$f_{ed} = \frac{\nu}{(2J+1)}\left[\frac{8\pi^2 mc}{3h}\frac{(n^2+2)^2}{9n}\right]\sum_{\lambda=2,4,6}\Omega_\lambda \left\langle \psi J \left\| U^\lambda \right\| \psi' J' \right\rangle^2 \qquad \dots (3)$$

where $(2J + 1)$ is the degeneracy of the ground state, ν is the mean energy of the $\left|\psi J\right\rangle \rightarrow \left|\psi' J'\right\rangle$ transition, U^λ is a unit tensor operator of rank λ and U^λ 's are parameters known as J-O intensity parameters. The values of the reduced matrix elements, $\left\| U^\lambda \right\|$, have been evaluated for the Dy^{3+} ion using the relation

$$\left\langle f^N \alpha SLJ \left\| U^\lambda \right\| f^N f^N \alpha' S' L' J' \right\rangle = (-1)^{S+J+L'+\lambda}\left[(2J+1)(2J'+1)\right]^{1/2} {}^{JJ'\lambda}_{L'LS}$$

$$\times \left\langle f^N \alpha SL \left\| U^\lambda \right\| f^N f^N \alpha' S' L' \right\rangle \qquad \dots (4)$$

The matrix elements and the 6j symbols required for the analysis have been taken from the literature [Carnaal *et al* 1978]. The matrix elements were then transformed from the LS basis state to the physical coupling scheme prior to being used in the calculation.

$|<||U^t||>|^2$ represents the square of the matrix elements of the unit tensor operator U^t connecting the initial and final states. The calculated values of JO parameters are given in Table 2. Once the Ω_λ quantities have been determined, they can subsequently be utilized to calculate the properties of transitions that have not been experimentally measured, including the radiative life time. The values of the radiative transition probability (A), total radiative transition probability (A_T), radiative life time (τ) fluorescence branching ratio (β_R) and the integrated absorption crossection for stimulated emission are evaluated using the expressions

$$A^{ed}{}_{JJ} = \frac{64\pi^2 e^2 \upsilon^3}{3h\left(2J+1\right)}\left[\frac{n\left(n^2+2\right)^2}{9}\right]S_{ed} \qquad \dots (5)$$

where

$$S_{ed} = \sum_{\lambda=2,4,6}\Omega_\lambda \left\langle \psi J \left\| U^\lambda \right\| \psi' J' \right\rangle^2 \qquad \dots (6)$$

As the coefficients for spontaneous emission equal the reciprocal radiative relaxation time, we have

$$A^{ed}_{JJ} = \tau^{-1}_{Rad} \qquad \dots (7)$$

or

$$\tau_{rad} = \frac{1}{\sum_{J'} A_{JJ'}} \qquad \dots (8)$$

The position of the lines in absorption or emission spectra seems to be independent of the surroundings. The relative amplitudes of the fluorescence transitions or fluorescence branching ratio is given by

$$\beta_{JJ'} = \frac{A_{JJ'}}{\sum_{J'} AJJ'} \qquad \ldots (9)$$

Branching ratio is the ratio of the radiative transition probability to the total radiative relaxation rate. It measures the percentage of emission for a given transition from a state with respect to all other transitions from this state. The integrated absorption cross-section or effective cross-section (σ_a) for stimulated emission is estimated using the Fuchtbauer–Landenberg equation.

$$\sigma_a = \frac{A(\psi J)}{8\pi c n^2 \upsilon^2} \qquad \ldots (10)$$

All the calculated values of radiative parameters are given in Table 3. From the table it is clear that the branching ratio and the stimulated absorption crossection is maximum for the $^4F_{9/2} \rightarrow {}^6H_{13/2}$ and $^4F_{9/2} \rightarrow {}^6H_{15/2}$ transitions and these transitions can be utilized for optical applications.

Table 2. Judd-Ofelt parameters of Dy^{3+} in silica matrices.

Matrix	**JO parameters (10^{-20} cm^2)**			**Order**
	Ω_2	**Ω_4**	**Ω_6**	
SiO$_2$	7.07	5.08	3.45	$\Omega_2>\Omega_4>\Omega_6$

Table 3. Calculated radiative parameters of Dy^{3+} ion in SiO$_2$ matrix

Transition from $^4F_{9/2}$	**Energy ν cm^{-1}**	**S$_{ed}$ (10^{-22} cm^2)**	**A s^{-1}**	**A$_T$ s^{-1}**	**τ$_{rad}$ μs**	**β**	**σ$_a$ (10^{-19}cm^2)**
$^6F_{1/2}$	7283	0.203	1	1239	807	0.001	0.091
$^6F_{3/2}$	7845	0.104	1			0.001	0.115
$^6F_{5/2}$	8649	5.144	8			0.006	0.647
$^6F_{7/2}$	10082	3.429	13			0.014	0.777
$^6H_{5/2}$	10892	2.293	7			0.005	0.353
$^6H_{7/2}$	11955	7.285	34			0.027	1.431
$^6F_{9/2}$	12039	3.634	19			0.015	0.795
$^6F_{11/2}$	13361	5.133	48			0.038	1.625
$^6H_{9/2}$	13390	4.017	29			0.023	9.797
$^6H_{11/2}$	15269	9.03	78			0.069	2.02
$^6H_{13/2}$	17670	64.59	743			0.599	14.49
$^6H_{15/2}$	21140	12.94	258			0.208	3.498

CONCLUSIONS

Dy^{3+} doped silica matrices were prepared by sol-gel process and the spectroscopic properties in dried gels and gel glasses were studied. Using the Judd-Ofelt parameters various radiative parameters such as radiative transition probability (*A*), total radiative transition probability (A_T), radiative life time (τ) fluorescence branching ratio (β_R) and the integrated absorption crossection for stimulated emission were evaluated. From the analysis it is clear that the $^4F_{9/2} \rightarrow {}^6H_{13/2}$ and $^4F_{9/2} \rightarrow {}^6H_{15/2}$ transitions can be utilized for optical amplification.

REFERENCES

1. Carnaal, W. T., Hessler, J. P., Wagner Jr. F., *J. Phys. Chem,* **83**, 2152 (1978).
2. Costa, V. C., Lochhead, M. J., Bray, K. L., *Chem. Mater.*, Vol. **8**, p.783 (1996).
3. Gijo, Jose, Jose, G, Joseph, C., Thomas, V., Unnikrishnan, N. V., Ittyachen, M. A., *Mater. Chem.Phys.*, Vol. **96**, p. 381 (2006).
4. Jayasankar, C. K., Rukmini, E., *Physica B,* **240**, 273 (1997).
5. Thomas, Jeena, George, A.V., Thomas, V., *Asian J. Chem.*, Vol. **25**, p. 6767 (2013).
6. Joanna, Pisarska, *Optica Applicata*, Vol. **XL,** p. 367 (2010).
7. Judd, B. R., *Phys, Rev.*, **127**, 750 (1962).
8. Maria, Czaja, Body, Sabina, Pisarska, Joanna Gabrys, Mazurak, Zbigniew, *Opt. Mater.*, Vol. **31**, p. 1898 (2009).
9. Ofelt, G. S., *J. Chem. Phys,* **37**, 511 (1962).
10. Paulose, P. I., Jose, G., Gijo, Jose, Thomas, V., Unnikrishnan, N. V., Warrier, M. K. R., *Bull. Mater. Sci.*, Vol. **25**, p. 69 (2002).
11. Thomas, I. M., Payne, S. A., Wilke, G. D., *J. Non-Cryst. Solids,* Vol. **151**, p. 183 (1992).
12. Thomas, V., Anit, Elizebeth, Thomas, H., Jose, G., Unnikrishnan, N. V., Cyriac, Joseph, Ittyachen, M. A., *J. Opto. Electro. Adv. Mater.*, **7**, 2687 (2005).
13. Thomas, Vinoy, Gijo, Jose, Rajagopal, S., Biju, P. R., Unnikrishnan, N. V., *J. Sol-Gel Sci. Tech.*, Vol. **33**, p. 269 (2005).
14. You, Zhou, Xiang-Hong, He, Bing, Yan, *Opt. Mater.*, Vol. **36**, p. 602 (2014).

❑